Nonequilibrium structures and dynamic transitions in driven vortex lattices with disorder

Alejandro B. Kolton* and Daniel Domínguez*

*Centro Atómico Bariloche and Instituto Balseiro, 8400 San Carlos de Bariloche, Argentina

Abstract. We review our studies of elastic lattices driven by an external force F in the presence of random disorder, which correspond to the case of vortices in superconducting thin films driven by external currents. Above a critical force F_c we find two dynamical phase transitions at F_p and F_t, with $F_c < F_p < F_t$. At F_p there is a transition from plastic flow to smectic flow where the noise is isotropic and there is a peak in the differential resistance. At F_t there is a sharp transition to a frozen transverse solid where both the transverse noise and the diffusion fall down abruptly and therefore the vortex motion is localized in the transverse direction. From a generalized fluctuation-dissipation relation we calculate an effective transverse temperature in the fluid moving phases. We find that the effective temperature decreases with increasing driving force and becomes equal to the equilibrium melting temperature when the dynamic transverse freezing occurs.

INTRODUCTION

The study of the collective motion of vortex lattices in superconductors has brought new concepts in the non-equilibrium statistical physics of driven disordered media [1, 2, 3, 4, 5, 6, 7, 8, 9, 10, 11, 12, 13]. The prediction by Koshelev and Vinokur [1] of a *dynamical phase transition* upon increasing drive, from a fluid-like flow regime [2, 3, 4] to a coherently moving solid [1], has motivated an outburst of theoretical [5, 6, 7, 8], experimental [9, 10, 11], and simulation [12, 13] work. The relevant physics of the high velocity driven phase is controlled by the transverse displacements (in the direction perpendicular to the driving force) [5], leading to a new class of driven systems characterized by *anisotropic spatial structures* with transverse periodicity [5, 6, 7]. These moving anisotropic vortex structures have been observed experimentally by Pardo *et al.* [11], and their different features have been studied in simulations [12, 13].

Koshelev and Vinokur [1] defined a "shaking" temperature $T_{\mathtt{sh}}$ from the fluctuating force felt by a vortex configuration moving in a random pinning potential landscape. This lead to their prediction of a dynamic phase transition when $T_{\mathtt{sh}}$ equals the equilibrium melting temperature of the vortex system [1]. This dynamic transition separates the liquid-like phase of vortices moving at low driving forces from the "crystalline" vortex lattice moving at large forces. However, later work [5, 6, 7] has shown that the perturbation theory used in [1] breaks down and that the vortex phase at large velocities can be an anisotropic transverse glass instead of a crystal. In spite of this, the shaking temperature introduced in [1] has been a useful qualitative concept, at least phenomenologically.

Cugliandolo, Kurchan and Peliti [14] have introduced the notion of time-scale dependent "effective temperatures" $T_{\mathtt{eff}}$ from a modification of the fluctuation-dissipation theorem (FDT) in slowly evolving out of equilibrium systems. $T_{\mathtt{eff}}$ is defined from the

slope of the parametric plot of the integrated response against the correlation function of a given pair of observables when the latter is bounded or, equivalently, it is the inverse of twice the slope of the parametric plot of the integrated response against the displacement when the correlation is unbounded. This definition yields a bona fide temperature in the thermodynamic sense since it can be measured with a thermometer, it controls the direction of heat flow for a given time scale and it satisfies a zero-th law within each time scale. $T_{\mathtt{eff}}$ was found analytically in mean-field glassy models [15] and it was successfully studied in structural and spin glasses, both numerically [16] and experimentally [17], in granular matter [18] and in weakly driven sheared fluids [19].

In this article, we will review our work on the dynamical regimes and nonequilibrium transitions of the driven vortex lattices as a function of the driving force [13], and show how an adequate definition of an effective temperature (based on Ref. [14]) can help to understand these phenomena [20].

MODEL

The equation of motion of a vortex in position $\mathbf{r}_i$ is:

$$\eta \frac{d\mathbf{r}_i}{dt} = -\sum_{j\neq i} \nabla_i U_v(r_{ij}) - \sum_p \nabla_i U_p(r_{ip}) + \mathbf{F} + \zeta_{\mathbf{i}}(\mathbf{t}) \tag{1}$$

where $r_{ij} = |\mathbf{r}_i - \mathbf{r}_j|$ is the distance between vortices i, j, $r_{ip} = |\mathbf{r}_i - \mathbf{r}_p|$ is the distance between the vortex i and a pinning site at $\mathbf{r}_p$, $\eta = \frac{\Phi_0 H_{c2} d}{c^2 \rho_n}$ is the Bardeen-Stephen friction and $\mathbf{F} = \frac{d\Phi_0}{c}\mathbf{J}\times\mathbf{z}$ is the driving force due to an applied current $\mathbf{J}$. In two-dimensional superconductor the vortex-vortex interaction potential is logarithmic: $U_v(r) = -A_v \ln(r/\Lambda)$, with $A_v = \Phi_0^2/8\pi\Lambda$ [3]. The vortices interact with a random uniform distribution of attractive pinning centers with $U_p(r) = -A_p e^{-(r/r_p)^2}$ with r_p being the coherence length. We normalize length scales by r_p, energy scales by A_v, and time is normalized by $\tau = \eta r_p^2/A_v$. The effect of a thermal bath at temperature T is given by the stochastic force $\zeta_i(t)$, satisfying $\langle \zeta_i^\mu(t)\rangle = 0$ and $\langle \zeta_i^\mu(t)\zeta_j^{\mu'}(t')\rangle = 2\eta k_B T \delta(t-t')\delta_{ij}\delta_{\mu\mu'}$. We consider N_v vortices and N_p pinning centers in a rectangular box of size $L_x \times L_y$, and the normalized vortex density is $n_v = N_v r_p^2/L_x L_y = B r_p^2/\Phi_0$. Moving vortices induce a total electric field $\mathbf{E} = \frac{B}{c}\mathbf{v}\times\mathbf{z}$, with $\mathbf{v} = \frac{1}{N_v}\sum_i \mathbf{v}_i$. We use periodic boundary conditions and the periodic long-range logarithmic interaction is evaluated with an exact and fast converging sum [21]. Typical simulation parameters correspond to vortex densities of $n_v = 0.05 - 0.12$ in a box with $L_x/L_y = \sqrt{3}/2$, with $N_v = 64 - 784$, pinning strengths of $A_p/A_v = 0.1 - 0.35$, and densities of pinning centers $n_p > n_v$ (dense pinning $n_p > n_v$, is typically realized in experimental samples). The equations are integrated with a time step of $\Delta t = 0.01 - 0.1\tau$ and averages are evaluated in $30000 - 80000$ integration steps after $2000 - 30000$ iterations for equilibration (when the total energy reaches a stationary value).

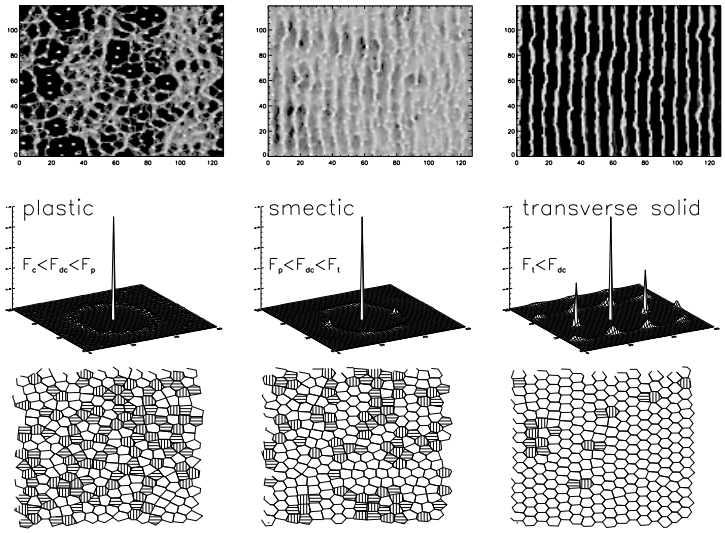

FIGURE 1. Examples of steady states for different dynamical regimes. Upper panel: Vortex trajectories. Middle pannel: Average structure factor $S(\mathbf{k})$. Lower pannel: Voronoi construction for each given vortex structure.

DYNAMICAL REGIMES

We start by showing the vortex trajectories and their translational order in the different steady state regimes. In the upper panel of Fig. 1 we show the vortex trajectories $\{\mathbf{r}_i(t)\}$ for typical values of F by plotting all the positions of the vortices for all the time iteration steps. We also study the time-averaged structure factor $S(\mathbf{k}) = \langle|\frac{1}{N_v}\sum_i \exp[i\mathbf{k}\cdot\mathbf{r}_i(t)]|^2\rangle$, which is shown in the middle pannel of Fig. 1. The number of deffects in the lattice structure can be obtained from a Voronoi construction. This in shown in the lower pannel of Fig. 1, where the lattice defects are shown in gray. In Fig. 2(a) we plot the average vortex velocity $V = \langle V_y(t)\rangle = \langle\frac{1}{N_v}\sum_i \frac{dy_i}{dt}\rangle$, in the direction of the force as a function of F and its corresponding derivative dV/dF. Below a critical force F_c all the vortices are pinned and there is no motion, $V = 0$. Above F_c, we can distinguish three different dynamical regimes:

(i) Plastic flow: $F_c < F < F_p$. At F_c vortices start to move in a few filamentary channels [3]. A typical situation is shown in Fig. 1, where a fraction of the vortices are moving in an intricate network of channels. As the force is increased a higher fraction of vortices is moving. In this regime, vortices can move in the transverse direction (perpendicular to **F**) through the tortuous structure of channels [4]. We see that the corresponding $S(\mathbf{k})$ only has the central peak showing the absence of ordering in this plastic flow regime [2, 3, 4] and that there are a large number of defects.

(ii) Smectic flow: $F_p < F < F_t$. We find a peak in the differential resistance, dV/dF, at a characteristic force F_p. At $F = F_p$ we see that *all* the vortices are moving in a seemingly isotropic channel network with maximum interconnectivity. In the experiment of Hellerqvist *et al* [10] the value of F_p was taken as an indication of a dynamical phase transition. In fact, we find that above F_p a new dynamic regime sets in. In this case, as

we show in Fig. 1, all the vortices are moving in trajectories that are mostly parallel to the force, forming "elastic channels". Two small Bragg peaks appear in the structure factor along the $K_y = 0$ axis, which correspond to $\mathbf{G}_1 = (\pm 2\pi/a_0, 0)$. This is consistent with the onset of "smectic" ordering [6] in the transverse direction with elastic channels separated by a distance $\sim a_0 = n_v^{-1/2}$. In this regime the transverse motion consists in vortex jumps from one channel to another, resembling "thermally" activated transitions induced by local chaos. The rate of these transitions decreases with increasing force. In Fig. 2(b) we plot the magnitude of the Bragg peaks at G_1, $S_s = S(G_1)$, corresponding to smectic ordering ($K_y = 0$), and the other neighboring peaks at $\mathbf{G}_2 = \pm 2\pi/a_0(1/2, \sqrt{3}/2)$ and $\mathbf{G}_3 = \pm 2\pi/a_0(-1/2, \sqrt{3}/2)$, $S_l = (S(G_2) + S(G_3))/2)$, corresponding to longitudinal ordering ($K_y \neq 0$). We see that above F_p the intensity of the smectic peak S_s starts to grow and $S_s \gg S_l$, while below F_p the spatial structure is isotropic, $S_s = S_l \ll 1$. The Bragg peak heights depend with system size as $S(G) \sim N_v^{-\sigma_G}$, where $\sigma_G = 0$ means long-range order (LRO), $0 < \sigma_G < 1$ means quasi long-range order (QLRO) and $\sigma_G \geq 1$ means short-range order (SRO). We have found that $\sigma_G \geq 1$ in this regime: there is only short range smectic order [13], and thus this phase corresponds to a fluid. In this sense the transition at F_p is a dynamic transition in the flow.

(iii) Frozen transverse solid: $F > F_t$. At a new characteristic force F_t, the jumps between channels suddenly stop and vortex motion becomes frozen in the direction perpendicular to $\mathbf{F}$. An example for $F > F_t$ is shown in Fig. 1 where we see well defined elastic channels parallel to $\mathbf{F}$. We see that new peaks appear in $S(\mathbf{k})$ in directions with $K_y \neq 0$, like G_2, G_3, showing that there is some longitudinal ordering between the channels. These extra peaks are smaller than the smectic peaks, and $S(\mathbf{k})$ is very anisotropic. We note in Fig. 2(a) that F_t is the point where the noisy behavior in dV/dF ceases. A similar criterion was used by Bhattacharya and Higgins to define their dynamical phase diagram [9]. In Fig. 2(b) we see that in F_t there is an increase in the longitudinal ordering S_l, and both S_s and S_l tend to saturate at an almost constant value for $F \gg F_t$. Furthermore, we have we found that there is QLRO with a value of $0.5 < \sigma_G < 0.7$ [13]. We also see that in this phase there are very few defects, corresponding to dislocations oriented in the direction of the force.

DYNAMICAL TRANSITIONS

An understanding of the *dynamical* transitions can be obtained from studying the temporal behavior of the system. It has been observed experimentally that the longitudinal voltage can show low frequency noise. This voltage noise reaches a very large value above the critical current, which has been attributed to plastic flow, and then the noise decreases for large current. In addition, even when the total dc transverse voltage $\langle V_x \rangle = \langle \frac{1}{N_v} \sum_i \frac{dx_i}{dt} \rangle$ is zero, it can also have fluctuations and noise. In fact, it is easy to understand that this transverse noise will be closely related to the wandering and wiggling of the plastic flow channels and to the jumps between elastic channels in the smectic phase. We have calculated in [13] the power spectrum of both the longitudinal voltage and the transverse voltage. We have found [13] that near the critical force, the longitudinal noise, P_y, is larger than the transverse noise, P_x. At F_p the voltage noise becomes isotropic,

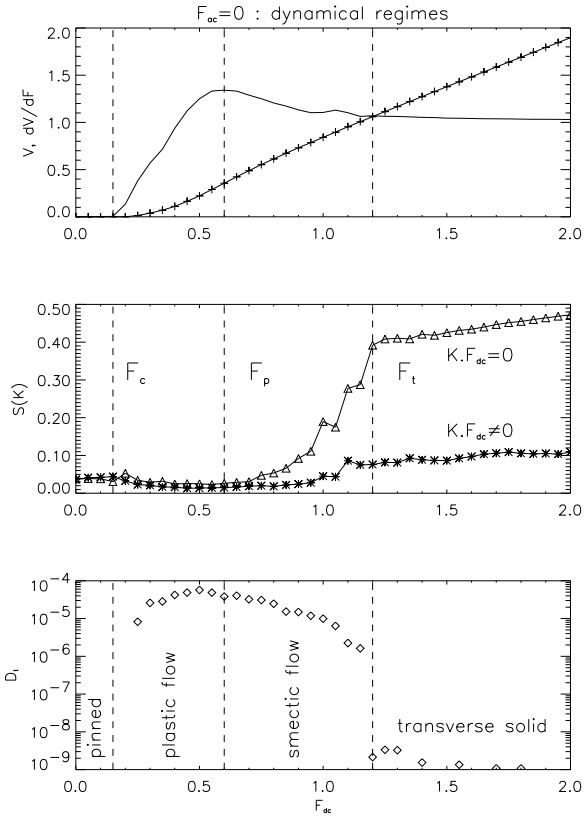

FIGURE 2. (a) Velocity-force curve (voltage-current characteristics), + symbols. dV/dF curve (differential resistance), continuous line. (b) Intensity of the Bragg peaks. For smectic ordering, $K_y = 0$: triangles; for longitudinal ordering, $K_y \neq 0$, asterisks. (c) Diffusion coefficient for transversal motion, D_x.

$P_x = P_y$. This is the point where we have seen the highest interconnection in the channel network. The coincidence of isotropic noise, onset of short-range smectic order and peak in differential resistance suggest that there is a dynamic transition at F_p. Above F_p, the onset of elastic channels and smectic ordering reduces the longitudinal noise, while the transverse noise remains large due to the "activated" jumps between elastic channels. At F_t the transverse noise falls abruptly, by several orders of magnitude. This corresponds to a *freezing transition* of vortex motion in the transverse direction. Above F_t there are no more vortex jumps between elastic channels. The low frequency noise can be closely related to diffusive motion for large times. We have analyzed the average quadratic displacements of vortices in the transverse direction from their center of mass position $(X_{cm}(t), Y_{cm}(t))$ as a function of time. We define $w_x(t) = \frac{1}{N_v}\sum_i [\tilde{x}_i(t) - \tilde{x}_i(0)]^2$, where $\tilde{x}_i(t) = x_i(t) - X_{cm}(t)$. We have found that the vortex motion in the fluid regimes, for $F_c < F < F_t$, is diffusive in the transverse direction, with $w_x(t) \sim D_x t$. In Fig. 2(c) we show the behavior of the transverse diffusion coefficient D_x. The transverse diffusion is maximum at the peak in the differential resistance, F_p, and it has a clear and abrupt jump to zero at F_t indicating the transverse freezing transition. It is interesting to note that melting transitions also show a jump in the diffusion coefficient.

EFFECTIVE TEMPERATURE

To study the fluctuation-dissipation relation (FDR), we proceed in a similar way as in simulations of structural glasses [16] and consider the observables:

$$A_\mu(t) = \frac{1}{N_v}\sum_{i=1}^{N_v} s_i r_i^\mu(t)\,; \quad B_\mu(t) = \sum_{i=1}^{N_v} s_i r_i^\mu(t)\,, \tag{2}$$

where $s_i = -1, 1$ are random numbers with $\overline{s_i} = 0$ and $\overline{s_i s_j} = \delta_{ij}$, and $r_i^\mu = R_i^\mu - R_{cm}^\mu$ with $\mu = x,y$ and $\mathbf{R}_{cm}$ being the center of mass coordinate. Taking $\mathbf{F} = F\mathbf{y}$ we study separately the FDR in the transverse and parallel directions with respect to $\mathbf{F}$. The time correlation function between the observables A_μ and B_μ is

$$C_\mu(t,t_0) = \overline{\langle A_\mu(t) B_\mu(t_0)\rangle} = \frac{1}{N_v}\sum_{i=1}^{N_v}\langle r_i^\mu(t) r_i^\mu(t_0)\rangle\,, \tag{3}$$

since the r_i^μ are independent of the s_i. The integrated response function χ_μ for the observable A_μ is obtained by applying a perturbative force $\mathbf{f}_i^\mu = \varepsilon s_i \hat{\mu}$ (where $\hat{\mu} = \hat{x},\hat{y}$) at time t_0 and keeping it constant for all subsequent times on each vortex:

$$\chi_\mu(t,t_0) = \lim_{\varepsilon\to 0}\frac{1}{\varepsilon}\left[\overline{\langle A_\mu(t)\rangle}_\varepsilon - \overline{\langle A_\mu(t)\rangle}_{\varepsilon=0}\right]. \tag{4}$$

We then define a function, $T_{\mathtt{eff}}^\mu(t,t_0)$, by the relation,

$$\chi_\mu(t,t_0) = \frac{1}{2k_B T_{\mathtt{eff}}^\mu(t,t_0)}\Delta_\mu(t,t_0)\,, \tag{5}$$

where $\Delta_\mu(t,t_0) = \frac{1}{N_v}\sum_{i=1}^{N_v}\langle |r_i^\mu(t) - r_i^\mu(t_0)|^2\rangle = C_\mu(t,t) + C_\mu(t_0,t_0) - 2C_\mu(t,t_0)$ is the quadratic mean displacement in the direction of $\hat{\mu}$. For a system in equilibrium at temperature T the FDT requires that $T_{\mathtt{eff}}^x = T_{\mathtt{eff}}^y = T$. In a nonequilibrium system, like the driven vortex lattice with pinning, the FDT does not apply. Since we are interested in the *stationary* states reached by the driven vortex lattice, where aging effects are stopped [19], then all observables depend only on the difference $t - t_0$, if we choose t_0 long enough to ensure stationarity. From the parametric plot of $\chi_\mu(t)$ vs. $\Delta_\mu(t)$ one defines the effective temperature $T_{\mathtt{eff}}^\mu(t)$ using Eq. (5), provided $T_{\mathtt{eff}}^\mu(t)$ is a constant in each time-scale [14].

We have studied [20] the transverse and longitudinal FDR for the moving vortex lattice as a function of driving force, F, solving the dynamic equations for different values of A_p, n_v, and T within the fluid regimes, $F_c < F < F_t$. We have obtained [20] for each F parametric plots of the transverse quadratic mean displacements, $\Delta_x(t)$ as a function of the integrated transverse response, $\chi_x(t)$. We found that the equilibrium FDT does not apply in general but two approximate linear relations exist for $\Delta_x(t) < 0.05 r_p^2$ and for $\Delta_x(t) > r_p^2$, with a non-linear crossover between them. We have found that the short displacements region corresponds to the bath temperature, T, meaning that the

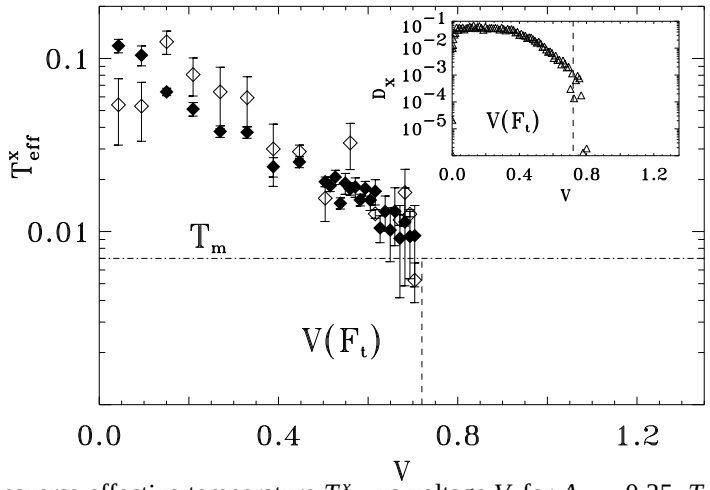

FIGURE 3. Transverse effective temperature $T^x_{\mathtt{eff}}$ vs voltage V for $A_p = 0.35$, $T = 0$ and $n_v = 0.07$, using the diffusion relation (filled diamonds) and a generalized Kubo formula (open diamonds). Inset: Transverse diffusion constant D_x vs V. Dashed lines indicate the transverse freezing transition at $F = F_t$ and the dash-dotted line indicate the melting temperature of the unpinned system $T_m \approx 0.007$.

equilibrium FDT applies in the transverse direction only for short times, $t \ll r_p/v$. For the large displacements region we have obtained a different slope corresponding to an effective transverse temperature $T^x_{\mathtt{eff}}(T) > T$. Furthermore, when comparing the results for different T, we have found $T^x_{\mathtt{eff}}(T) \approx T^x_{\mathtt{eff}}(0) + T$. On the other hand, a similar analysis of the FDR for the longitudinal direction does not show a constant slope for large displacements or long times such that $t > r_p/v$.

In Fig. 3 we show the transverse effective temperature obtained in Ref. [20], $T^x_{\mathtt{eff}}$, for $T = 0$ as a function of voltage (*i.e.*, average velocity, V). We observe that $T^x_{\mathtt{eff}}$ is a decreasing function of V. The most remarkable result is that $T^x_{\mathtt{eff}}$ reaches a value close to the equilibrium melting temperature of the unpinned system, $T_m \approx 0.007$ [22], when the system approaches the transverse freezing transition at $F = F_t$ (obtained from the vanishing of the transverse diffusion D_x, shown in the inset). We have found that $T^x_{\mathtt{eff}} \to T_m$ when $F \to F_t$ for different values of pinning amplitude, A_p, and vortex density, n_v, even when F_t depends on A_p, n_v.

CONCLUSIONS

In conclusion, we have obtained evidence of two dynamical phase transitions. The first transition at F_p is the point of isotropic noise and maximum transverse diffusion and corresponds to the observed peak in the differential resistance. The second transition at F_t is a freezing transition in the *transverse* direction, where the transverse diffusion vanishes abruptly. We have been able to define an effective temperature in the moving fluid phase, using the thermodynamically adequate definition of [14]. The fact that we find that dynamic freezing occurs when $T^x_{\mathtt{eff}}(T) = T_m$, clearly indicates that there is a nonequilibrium phase transition at F_t.

ACKNOWLEDGMENTS

The research work reviewed here is the result of collaborations with N. Gronbech-Jensen, L. Cugliandolo and R. Exartier. Our work in Argentina has been supported by ANPCYT (grants PICT97-03-00121-02151, PICT97-03-00000-01034, PICT99-03-06343), by Fundación Antorchas (grant A-13532/1-96), Conicet (grant PIP-4946/96) and CNEA (within program P-5). A.B.K is also supported by a fellowship from Conicet.

REFERENCES

1. Koshelev, A. E., and Vinokur, V. M., *Phys. Rev. Lett.* **73**, 3580 (1994).
2. Jensen, H. J., et al., *Phys. Rev. Lett.* **60**, 1676 (1988); Shi, A.-C., and Berlinsky, A. J., *Phys. Rev. Lett.* **67**, 1926 (1991); Koshelev, A. E., *Physica C* **198**, 371 (1992); Faleski, M. C., et al., *Phys. Rev. B* **54**, 12427 (1996); Reichhardt, C., et al., *Phys. Rev. Lett.* **78**, 2648 (1997).
3. Grønbech-Jensen, N. , Bishop, A. R., and Domínguez, D. , *Phys. Rev. Lett.* **76**, 2985 (1996).
4. Olson, C. J. , Reichhardt, C., and Nori, F. , *Phys. Rev. Lett.* **80**, 2197 (1998).
5. Giamarchi, T., and Le Doussal, P. , *Phys. Rev. Lett.* **76**, 3408 (1996); Le Doussal, P., and Giamarchi, T. , *Phys. Rev. B* **57**, 11356 (1998).
6. Balents, L. , Marchetti, M. C., and Radzihovsky, L. , *Phys. Rev. B* **57**, 7705 (1998).
7. Scheidl, S., and Vinokur, V. M. , *Phys. Rev. E* **57**, 2574 (1998); *Phys. Rev. B* **57**, 13800 (1998).
8. Balents, L., and Fisher, M.P.A. , *Phys. Rev. Lett.* **75**, 4270 (1995).
9. Bhattacharya, S., and Higgins, M. J., *Phys. Rev. Lett.* **70**, 2617 (1993); Higgins, M. J., and Bhattacharya, S., *Physica C* **257**, 232 (1996).
10. Hellerqvist, M. C., et al., *Phys. Rev. Lett.* **76**, 4022 (1996).
11. Pardo, F., et al., *Nature (London)* **396**, 348 (1998).
12. Moon, K., et al., *Phys. Rev. Lett.* **77**, 2778 (1996); Ryu, S. et al., *Phys. Rev. Lett.* **77**, 5114 (1996); Spencer, S., and Jensen, H. J. , *Phys. Rev. B* **55**, 8473 (1997); Domínguez, D., et al., *Phys. Rev. Lett.* **78**, 2644 (1997); Olson, C. J., et al., *Phys. Rev. Lett.* **81**, 3757 (1998); Domínguez, D. , *Phys. Rev. Lett.* **82**, 181 (1999).
13. Kolton, A. B., et al., *Phys. Rev. Lett.* **83**, 3061 (1999); *Phys. Rev. B* **62**, R14657 (2000); *Phys. Rev. Lett.* **86**, 4112 (2001).
14. Cugliandolo, L. F. , Kurchan, J., and Peliti, L. , *Phys. Rev. E* **55**, 3898 (1997). Cugliandolo, L. F., and Kurchan, J. , *J. Phys. Soc. Japan* **69**, 247 (2000).
15. Cugliandolo, L. F., and Kurchan, J. , *Phys. Rev. Lett.* **71**, 173 (1993); *J. Phys. A* **27**, 5749 (1994).
16. Franz, S., and Rieger,H. , *J. Stat. Phys.* **79**, 749 (1995). Parisi, G. , *Phys. Rev. Lett.* **79**, 3660 (1997). Barrat, J.-L., and Kob, W. , *Europhys. Lett.* **46**, 637 (1999). Di Leonardo, R., et al., *Phys. Rev. Lett.* **84**, 6054 (2000).
17. Grigera, T. S., and Israeloff, N. , *Phys. Rev. Lett.* **83**, 5038 (1999); Bellon, L., et al., *Europhys. Lett.* **53**, 511 (2000). Herisson, D., and Ocio, M. , cond-mat/0112378.
18. Barrat, A., et al, *Phys. Rev. Lett.* **85**, 5034 (2000). Maske, H., and Kurchan, J. , *Nature* **415**, 614 (2002). Barrat, A., et al., cond-mat/0205285.
19. Berthier, L. , Barrat, J.-L., and Kurchan, J. , *Phys. Rev. E* **61**, 5464 (2000). Barrat, J.-L., and Berthier, L. , *Phys. Rev. E* **63**, 012503 (2001); Berthier, L., and Barrat, J.-L. , *J. Chem. Phys.* **116**, 6228 (2002).
20. Kolton, A.B. , Exartier, R. , Cugliandolo, L. , Domínguez, D., Gronbech-Jensen, N., cond-mat/0206042.
21. Grønbech-Jensen, N., *Int. J. Mod. Phys. C* **7**, 873 (1996); *Comp. Phys. Comm.* **119**, 115 (1999).
22. Caillol, J. M., et al., *J. Stat. Phys.* **28**, 325 (1982).